

available at [www.sciencedirect.com](http://www.sciencedirect.com)[www.elsevier.com/locate/scitotenv](http://www.elsevier.com/locate/scitotenv)

# Atmospheric mercury depletion event study in Ny-Alesund (Svalbard) in spring 2005. Deposition and transformation of Hg in surface snow during springtime

Christophe P. Ferrari<sup>a,b,\*</sup>, Cyril Padova<sup>a</sup>, Xavier Faïn<sup>a</sup>, Pierre-Alexis Gauchard<sup>a</sup>, Aurélien Dommergue<sup>a,b</sup>, Katrine Aspmo<sup>c,d</sup>, Torunn Berg<sup>c</sup>, Warren Cairns<sup>e</sup>, Carlo Barbante<sup>e,f</sup>, Paolo Cescon<sup>e,f</sup>, Lars Kaleschke<sup>g</sup>, Andreas Richter<sup>h</sup>, Folkard Wittrock<sup>h</sup>, Claude Boutron<sup>a,i</sup>

<sup>a</sup>Laboratoire de Glaciologie et Géophysique de l'Environnement du C.N.R.S., 54 rue Molière, BP 96, 38402 Saint Martin d'Hères, France

<sup>b</sup>Polytech' Grenoble, Université Joseph Fourier (Institut Universitaire de France), 28 Avenue Benoît Frachon, BP 53, 38041 Grenoble, France

<sup>c</sup>Norwegian Institute for Air Research (NILU), Instituttveien 18, P.O. Box 100, N-2027, Kjeller, Norway

<sup>d</sup>Department of Chemistry, University of Oslo, P.O. Box 1033, Oslo, Norway

<sup>e</sup>Instituto per la Dinamica dei Processi Ambientali del CNR, Dorsoduro, 2137, 30123, Venice, Italy

<sup>f</sup>Environmental Sciences Department, University of Venice, Calle Larga S. Marta, 2137, I-30123 Venice, Italy

<sup>g</sup>Institute of Oceanography, University of Hamburg, Germany

<sup>h</sup>Institute of Environmental Physics, University of Bremen, Germany

<sup>i</sup>Unités de Formation et de Recherche de Mécanique et de Physique, Université Joseph Fourier, BP 68, 38041 Grenoble, France

## ARTICLE INFO

### Article history:

Received 28 June 2007

Received in revised form

22 January 2008

Accepted 30 January 2008

Available online 8 April 2008

### Keywords:

Mercury

Snow

Deposition

Chemical transformation

AMDEs

## ABSTRACT

A field campaign was conducted in Ny-Ålesund (78°54'N, 11°53'E), Svalbard (Norway) during April and May 2005. An Atmospheric Mercury (Hg) Depletion Event (AMDE) was observed from the morning of April 24 until the evening of April 27. Transport of already Hg and ozone (O<sub>3</sub>) depleted air masses could explain this observed depletion. Due to a snowfall event during the AMDE, surface snow Hg concentrations increased two fold. Hg deposition took place over a short period of time corresponding to 3–4 days. More than 80% of the deposited Hg was estimated to be reemitted back to the atmosphere in the days following the event. During the campaign, we observed night and day variations in surface snow Hg concentrations, which may be the result of gaseous elemental mercury (GEM) oxidation to divalent Hg at the snow/air interface by daylight surface snow chemistry. Finally, a decrease in the reactive Hg (Hg<sub>R</sub>) fraction of total Hg (Hg<sub>T</sub>) in the surface snow was observed during spring. We postulate that the transformation of Hg<sub>R</sub> to a more stable form may occur in Arctic snow during spring.

© 2008 Elsevier B.V. All rights reserved.

## 1. Introduction

Mercury (Hg) is emitted to the atmosphere by both natural and anthropogenic sources (Munthe et al., 2001) and can then be

largely dispersed in the atmospheric reservoir. Gaseous elemental mercury (GEM) is the main mercury species in the atmosphere, with an average concentration of about 1.7 ng/m<sup>3</sup> (Slemr et al., 2003). Reactive gaseous mercury (RGM) and

\* Corresponding author. Present address: Laboratoire de Glaciologie et Géophysique de l'Environnement (L.G.G.E.), 54, rue Molière, 38402 Saint-Martin d'Hères, France. Tel.: +33 4 76 82 42 39; fax: +33 4 76 82 42 01.

E-mail address: [ferrari@lgge.obs.ujf-grenoble.fr](mailto:ferrari@lgge.obs.ujf-grenoble.fr) (C.P. Ferrari).

particulate mercury (PM) can be emitted directly by combustion sources (coal, waste incineration) or be formed through atmospheric GEM oxidation (Slemr et al., 1985; Lindberg and Stratton, 1998). This phenomenon, called Atmospheric Mercury Depletion Event (AMDE), has been observed mainly in polar atmospheres (Lu et al., 2001; Poissant and Pilote, 2001; Steffen et al., 2002; Lindberg et al., 2002; Ebinghaus et al., 2002; Temme et al., 2003; Berg et al., 2003; Skov et al., 2004; Sommar et al., 2004; Steffen et al., 2004; Gauchard et al., 2005). The oxidation chemistry is the result of halogen radicals and mainly bromine chemistry (Lindberg et al., 2002; Fain et al., 2006). GEM lifetime during a depletion event is about 4 h as compared to a normal lifetime of about one year. AMDEs can result from local, regional and/or long distance chemistry (Gauchard et al., 2005). The oxidation of GEM and subsequent formation of RGM and PM has, in some cases, led to elevated Hg deposition onto snow surfaces (Lu et al., 2001), while in other cases, no real increase in snow surface Hg levels was observed (Ferrari et al., 2005). This possible snow surface Hg deposition depends on the source of the AMDE, i.e. whether it is generated locally or due to already depleted air masses. Hg contained in snow can be reemitted back to the atmosphere via photochemical processes (Lalonde et al., 2002; Dommergue et al., 2003; Ferrari et al., 2005) or introduced into the ecosystem during snow melt. In this paper, we present the results of a springtime field campaign held in Ny-Ålesund (Svalbard) in 2005. The focal point of our study was to monitor atmospheric Hg speciation in order to determine the origin of the long AMDE recorded in April 2005. We also monitored snow surface Hg deposition during the event, as well as the stability of Hg complexes in surface snow during spring. Springtime Hg re-emission from the snow pack was also investigated so as to better understand the environmental parameters controlling this emission and the real impact of this process on the Arctic Hg snow budget.

## 2. Material and methods

### 2.1. Sampling locations

Two field sites were chosen around the Ny-Ålesund (78°54'N, 11°53'E) International Research and Monitoring Facility. Ny-Ålesund is a small settlement located on the west coast of Spitsbergen (Norway) which is the largest of the Svalbard islands (Fig. 1). The majority of the measurements took place in a small (~6 m<sup>2</sup>) electrically heated plywood shed located 300 m east of Ny-Ålesund, approximately 100 m from the seashore at 8 m.a.s.l. Data were also obtained from the Zeppelin Norway Research Station. This station is located 2 km south of Ny-Ålesund on a ridge of the Zeppelin Mountain at 474 m.a.s.l. The study started on April 18, 2005 and finished on May 14, 2005.

### 2.2. Atmospheric measurements

#### 2.2.1. GEM

Measurement of GEM was carried out at the heated plywood shed using a Tekran gas-phase mercury vapor analyzer (Model 2537A, Tekran Inc. Canada). The analytical technique, also



**Fig. 1 – Location of Svalbard, Norway. The field campaign took place in Ny-Ålesund, North-East of the major Island.**

called Cold Vapor Atomic Fluorescence Spectrophotometry (CVAFS), is based on collection of ambient mercury onto gold traps, followed by thermal desorption and final detection by atomic fluorescence spectrometry. The time resolution was 5 min, the sampling flow rate was 1.5 L/min and the analyzer was auto-calibrated daily.

#### 2.2.2. Ozone (O<sub>3</sub>)

O<sub>3</sub> was monitored at Zeppelin station using UV detection with a 49C analyzer (Thermo, United States). A previous study (Gauchard et al., 2005) demonstrated that both field sites (Zeppelin and Ny-Ålesund) yielded identical results for O<sub>3</sub> and GEM concentrations.

#### 2.2.3. RGM/PM

RGM and PM were measured at Ny-Ålesund between one and four times per day using manual methods described in Aspmo et al. (2005). RGM and PM were collected on KCl-coated annular denuder tubes and a KCl-coated quartz filter, respectively. Mercury species were thermally decomposed to GEM in a Hg-free air stream and subsequently analyzed by a Tekran 2537 unit.

### 2.3. Mercury in snow

#### 2.3.1. Cleaning procedure and snow sample collection

Most of the bottles used for snow collection were 25 mL PTFE bottles (some 50 mL and 250 mL bottles were also used) cleaned as described in Ferrari et al. (2005). Snow samples were collected every 12 or 24 h, depending on the weather at Ny-Ålesund, from a protected area with limited access. An integral non-emissive dust coverall and polyethylene gloves were used for snow collection. The bottles were

immediately placed into two polyethylene bags which were then hermetically sealed. Samples were stored in the dark at  $-20\text{ }^{\circ}\text{C}$  and transported frozen to the laboratory in Venice.

### 2.3.2. Snow sample analysis

Mercury analysis was conducted at the Department of Environmental Science of the University Ca'Foscari of Venice (Italy). Snow samples were melted in a cleanbench (Class 100) at ambient temperature and treated with 0.5% v/v ultra pure HCl before analysis. Reagents and water used were adapted for trace mercury measurements; therefore their Hg contribution was negligible. Two different analytical techniques, both based on the inductive coupled plasma mass spectrometer detection method, were carried out on snow samples. The first technique measured the reactive Hg ( $\text{Hg}_R$ ) concentration in snow samples (analysis with ICP-QMS Agilent series 7500) and the second, the total Hg ( $\text{Hg}_T$ ) concentration (analysis with ICP-SFMS Thermo Finnigan MAT Element 2; see Planchon et al., 2004).  $\text{Hg}_T$  includes complexes that are easily reducible by  $\text{SnCl}_2$  or  $\text{NaBH}_4$  such as  $\text{HgCl}_2$ ,  $\text{Hg}(\text{OH})_2$ ,  $\text{HgC}_2\text{O}_4$  (or  $\text{Hg}_R$ ) and stable complexes such as  $\text{HgS}$ ,  $\text{Hg}^{2+}$  bound to sulfur in humic compounds and some organo-mercuric species (Lindqvist and Rhode, 1985). The instruments were calibrated with Hg standards prepared from serial dilutions of a monoelemental  $\text{Hg}^{2+}$  solution with an initial concentration of  $1000\text{ mg ml}^{-1}$  (CPI International Santa Rosa, CA, USA). The Hg detection limit was  $0.18\text{ ng/L}$ , and the precision of the measurements was estimated to be 15% according to the relative standard deviation on five replicates.

### 2.4. GEM snow to air fluxes

A flux chamber coupled to a Tekran 2537A analyzer unit with a 10 min time resolution was used to measure GEM fluxes between the snow pack and ambient air at Ny-Ålesund. The chamber principle is based on the measurement of the difference between GEM concentrations inside and outside the chamber. Fluxes were calculated using the following equation:  $F = (\text{Ca} - \text{Ci}) * (\text{Q} / \text{A})$  where  $F$  is the flux in  $\text{ng/m}^2/\text{h}$ ,  $\text{Ca}$  is the GEM outlet concentration in  $\text{ng/m}^3$ ,  $\text{Ci}$  is the GEM inlet concentration in  $\text{ng/m}^3$ ,  $\text{Q}$  is the flushing flow rate in  $\text{m}^3/\text{h}$  ( $\sim 1.5\text{ L/min}$ ) and  $\text{A}$  is the area of the chamber, which is  $\sim 0.348\text{ m}^2$  (see Fain et al., 2007 for more details).

### 2.5. Other available parameters

#### 2.5.1. Meteorological data

Zeppelin station is part of the GAW (Global Atmospheric Watch) program directed by WMO (World Meteorological Organization), therefore meteorological measurements are carried out continuously on this site. Parameters such as irradiation, wind speed and direction, as well as temperature were provided for the study period.

#### 2.5.2. BrO

Atmospheric BrO columns can be determined from satellite measurements (e.g. Richter et al., 1998). These measure-

ments contain both the stratospheric and the tropospheric contribution. Since the stratospheric BrO field is relatively constant, enhanced BrO columns can be used as an indicator for increased boundary layer BrO concentrations. Here, we use maps of the BrO distribution retrieved from data obtained by the SCIAMACHY instrument on ENVISAT which are available at <http://www.iup.uni-bremen.de/does/>. BrO was measured at the Ny-Ålesund village with max-DOAS observation (see Wittrock et al., 2004; Wittrock, 2006).

#### 2.5.3. Frost flowers

Potential Frost Flower (PFF) coverage maps were provided by the University of Bremen (Germany). These maps were generated by a one dimensional thermodynamic model (initialized by satellite observations) which combines frost flower growth parameterization with sea ice heat equilibrium equations (see Kaleschke et al., 2004).

#### 2.5.4. Back trajectories

The back trajectories of air masses arriving at the Ny-Ålesund site were obtained via NOAA ARL (National Oceanic and Atmospheric Air Resources Laboratory). These back trajectories were generated with the Real-time Environmental Applications and Display system (READY) and compiled by the HYSPLIT (HYbrid Single-Particle Lagrangian Integrated Trajectory) model, which uses the atmospheric pressure recorded at the wind origin point and meteorological model data.

## 3. Results

### 3.1. Mercury and ozone

Fig. 2a and b shows the evolution of GEM and ozone concentrations from April 18 to May 6, 2005. An AMDE was recorded with a fast decrease in GEM and ozone. During the period from April 18 to April 24 (before 10:00), GEM and ozone concentrations were between  $1.5$  and  $1.9\text{ ng/m}^3$  and between  $80$  and  $100\text{ ppbv}$ , respectively. From April 24 at 10:00, ozone concentrations dropped to reach very low levels (around  $5\text{ ppbv}$ ) in less than 12 h. During the same time period, GEM concentrations decreased from  $\sim 1.66\text{ ng/m}^3$  (at 10:00) to  $\sim 0.25\text{ ng/m}^3$  (at 22:00). GEM and ozone concentrations remained low until April 26 at midnight, then increased slowly only to decrease again until April 27, 4:00. The depletion event lasted  $\sim 3.5$  days.

### 3.2. Particulate mercury (PM) and reactive gaseous mercury (RGM)

Fig. 2c and d shows the atmospheric PM and RGM concentrations at Ny-Ålesund from April 18 to May 6. Before the start of the GEM depletion, concentrations for both PM and RGM were below the detection limit of the apparatus ( $\sim 2\text{ pg/m}^3$  for RGM and  $\sim 3\text{--}5\text{ pg/m}^3$  for PM). PM peaked on April 25, with a concentration of about  $\sim 50\text{ pg/m}^3$ , while RGM peaked on April 27 with a concentration of about  $\sim 30\text{ pg/m}^3$ . PM concentrations decreased first

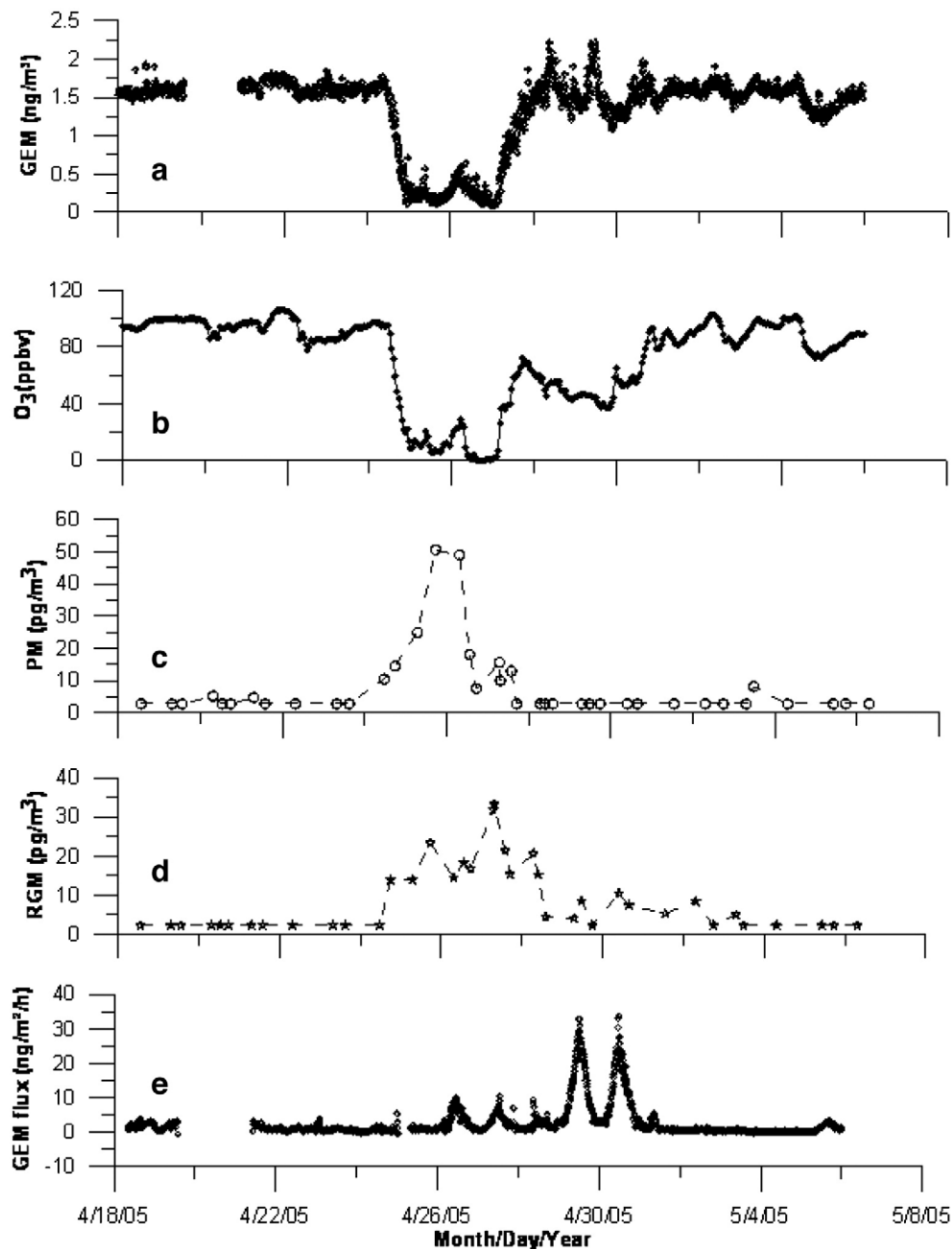


Fig. 2– (a) Ambient GEM concentrations ( $\text{ng}/\text{m}^3$ ), (b) Ozone concentrations (ppbv), (c) particulate mercury (PM) ( $\text{pg}/\text{m}^3$ ), (d) reactive gaseous mercury (RGM) ( $\text{pg}/\text{m}^3$ ), (e) GEM flux from the snow to the atmosphere ( $\text{ng}/\text{m}^2/\text{h}$ ), for April 18 to May 6, 2005 at Ny-Ålesund, Spitsbergen, Norway.

and reached background levels on April 27. RGM decreased more slowly and background levels were reached on April 29.

### 3.3. BrO at Ny-Ålesund

Fig. 3 shows the BrO concentration profile recorded from April 20 to April 30, 2005. Background levels were about 2 pptv before April 24 and increased suddenly to 12 pptv from April 24 to April 27. Background levels were reached after April 27.

### 3.4. Mercury in snow

Fig. 4 shows  $\text{Hg}_R$  and  $\text{Hg}_T$  concentrations in surface snow samples from April 18 to May 14, 2005. From April 18 to April 25,  $\text{Hg}_R$  concentrations ranged from 4 to 40  $\text{ng}/\text{L}$  and from 5 to 45  $\text{ng}/\text{L}$  for  $\text{Hg}_T$ . On April 26,  $\text{Hg}_R$  concentrations ranged from 30 to 60  $\text{ng}/\text{L}$  and  $\text{Hg}_T$  reached concentrations between 25 and 90  $\text{ng}/\text{L}$ . From April 27 to April 29,  $\text{Hg}_R$  concentrations dropped from 75 to ~15  $\text{ng}/\text{L}$  and never exceeded this value for the remainder of the campaign. For  $\text{Hg}_T$ , concentrations stayed high from May 4 to May 14. Regardless of the period,



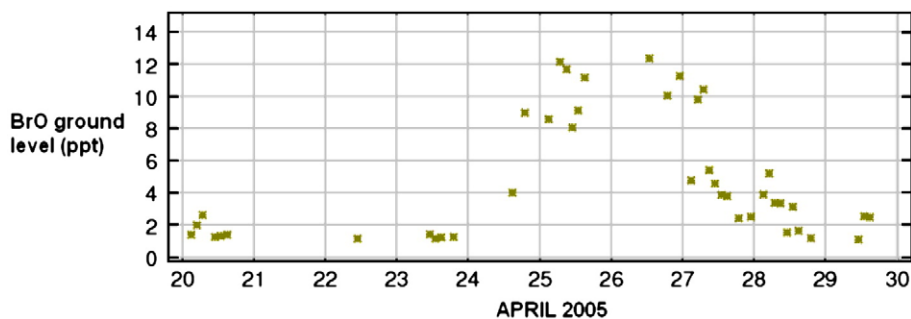


Fig. 3 – BrO concentrations recorded with max-DOAS at Ny-Ålesund from April 20 to April 30, 2005.

concentrations for both  $Hg_T$  and  $Hg_R$  were generally higher in the evening than early in the morning (see Table 1).

### 3.5. Snow to air exchange of gaseous elemental mercury

Fig. 2e shows snow to air GEM fluxes from April 18 to May 14, 2005. From April 18 to April 26 and from May 1 to May 14, fluxes never exceeded  $\sim 5$  ng/m<sup>2</sup>/h. For April 26, 27 and 28, GEM fluxes increased by a two fold factor ( $\sim 10$  ng/m<sup>2</sup>/h) and from April 29 and April 30, fluxes increased by factor of 7 ( $\sim 35$  ng/m<sup>2</sup>/h). Daily maximum fluxes were recorded near 12:00 and reached their minimum at night near 2:00.

## 4. Discussion

### 4.1. AMDE geographical and chemical origin

The ozone and GEM profiles and the air mass back trajectories show that there were three different periods during the AMDE: the beginning, the central period and the end, corresponding to three different air mass origins. Fig. 5 summarizes these

changes in air mass origin and GEM and ozone patterns. Fig. 6a, b and c (April 21 to 23) shows that in Ny-Ålesund, BrO levels were low, corresponding to a period with no ozone and Hg depletion (see Fig. 2a and b).

#### 4.1.1. AMDE beginning period

In order to understand whether this AMDE had a local or non-local origin,  $O_3$  apparent destruction rate ( $\Delta O_3/\Delta t$ ) was calculated during the event and compared to a theoretical rate obtained using a combined BrO–ClO mechanism for ozone destruction, as described in Tuckermann et al. (1997). For these authors, apparent destruction rates of  $\sim 4.5$  ppb/h or more can only be attributed to advection of air masses already depleted in  $O_3$ . Lower apparent destruction rates imply a stronger influence of chemistry, but during the AMDE in Ny-Ålesund, both phenomena occurred.

The decrease in  $O_3$  and GEM concentrations in April 24 could be explained by an arrival of already strongly depleted air masses for these chemical species. The  $O_3$  destruction rate ( $\Delta O_3/\Delta t$ ) was  $\sim 7.7$  ppb/h (Fig. 2b), which is clearly higher than 4.5 ppb/h, a value that characterizes AMDEs caused by already depleted air masses (Tuckermann et al., 1997). Furthermore, for April 24 and 25, SCIAMACHY data shows that the air was strongly concentrated in BrO between the northeast of Greenland and the northwest coast of Svalbard (see Figs. 3

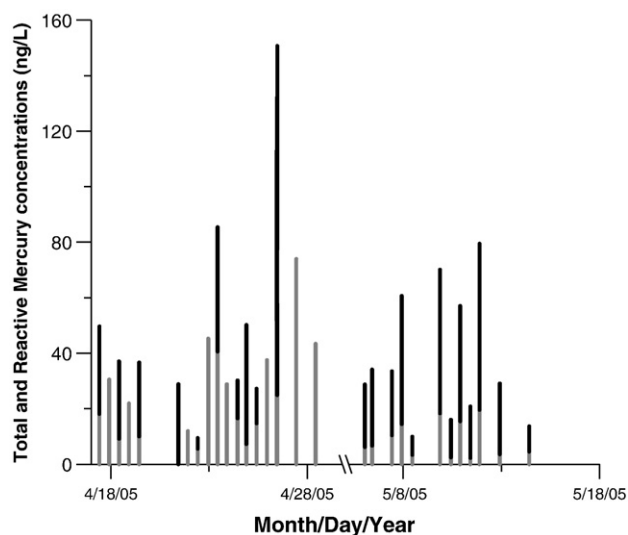
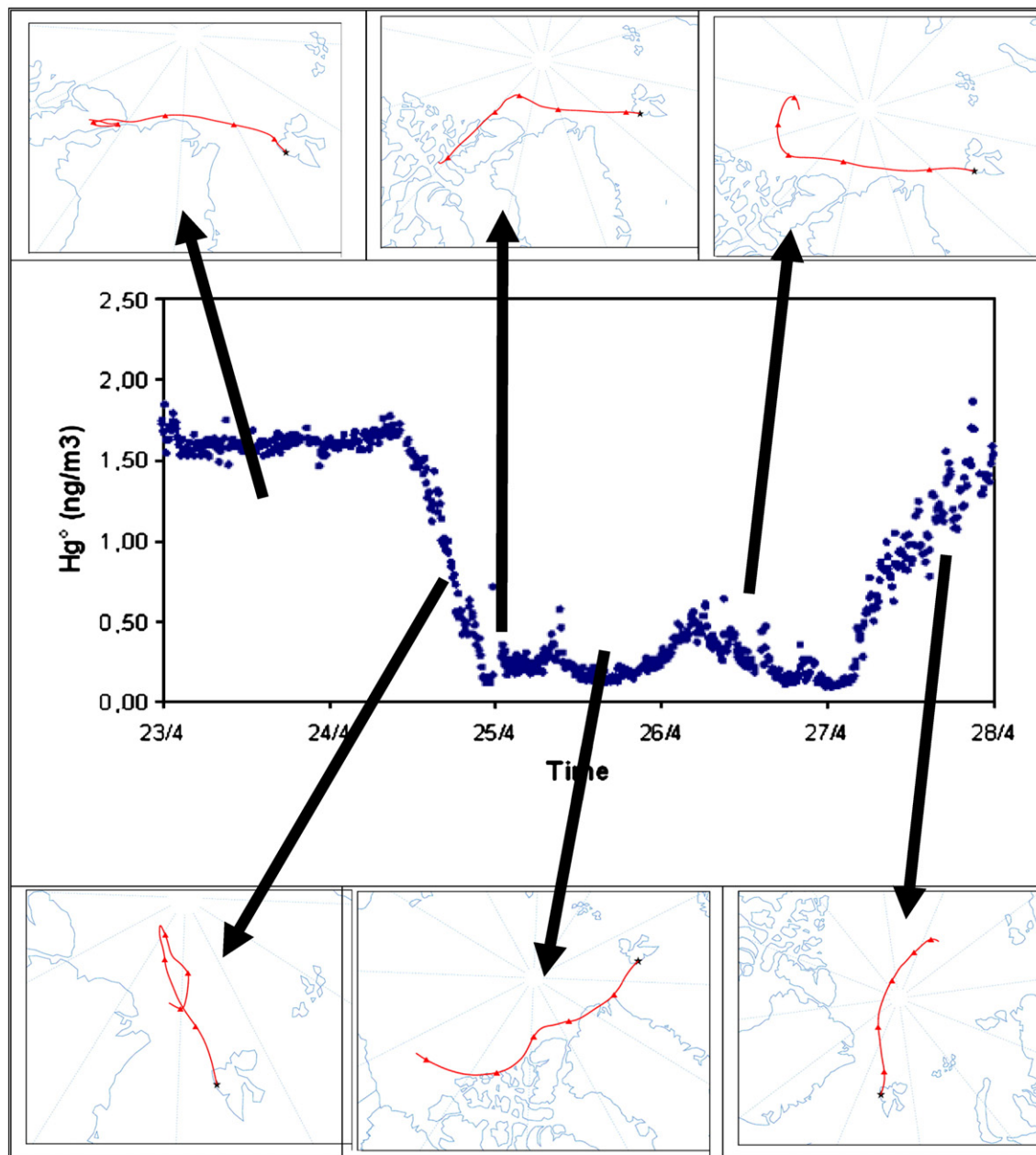


Fig. 4 –  $Hg_R$  and  $Hg_T$  concentrations (ng/L) in surface snow samples from Ny-Ålesund from April 18 to May 12, 2005. Grey lines correspond to  $Hg_R$  and black lines to  $Hg_T$ .

Table 1 –  $Hg_R$  and  $Hg_T$  concentrations in surface snow samples in the morning and the evening (ND = Not determined)

Date (Month/ Day/Year)	Morning concentrations (ng/L)		Evening concentrations (ng/L)	
	$Hg_R$	$Hg_T$	$Hg_R$	$Hg_T$
04/17/05	18.2	31.5	30.5	ND
04/18/05	9.2	27.9	21.9	ND
04/22/05	3.9	5.6	45.3	ND
04/23/05	40.6	44.8	28.9	ND
04/24/05	13.7	16.5	7.3	42.9
04/25/05	12.5	14.8	37.5	ND
05/04/05	1.9	9.3	14.6	58.9
05/05/05	1.4	12.3	6.2	22.6
05/07/05	10.5	23.1	14.5	46.2
05/10/05	2.5	13.6	15.5	41.6
05/11/05	2.2	18.6	19.6	59.9



**Fig. 5 – Temporal trends of GEM and ozone as well as back trajectories (over 120 h) of the air masses arriving at Ny-Ålesund from April 24 to April 27, 2005.**

and 6d and e). However, back trajectories arriving at 8:00 (before the onset of the AMDE) and at 16:00 (when the AMDE has started) differed in their direction (north coast of Greenland and the North Pole, respectively) and altitude (less elevated for the second, indicating a possible enrichment by active bromine compounds originating from the emission of the open sea). The depletion observed here could then be the result of transport of already depleted air masses.

#### 4.1.2. AMDE central period

During two days (from April 25 at 0:00 to April 27 at 0:00),  $O_3$  and GEM concentrations remained generally very low with some periodic increases (the morning of April 25 and April 26

at night). The back trajectories demonstrate that air masses arriving at the measurement site during these 2 days had the same geographical origin (northeast of Greenland). They bordered the north coast of Greenland before crossing over the Greenland Sea and arriving at Svalbard. Yet during some periods, some air masses flew over the Queen Elizabeth Islands and Ellesmere Island while others came from the Arctic Glacial Ocean. These air masses arrived at Ny-Ålesund with low GEM concentrations because they had previously flown over areas with high BrO concentrations, thus enabling GEM oxidation (see Fig. 6e and f). The low GEM and  $O_3$  concentrations could therefore be explained by regional or large scale transport of already depleted air masses.

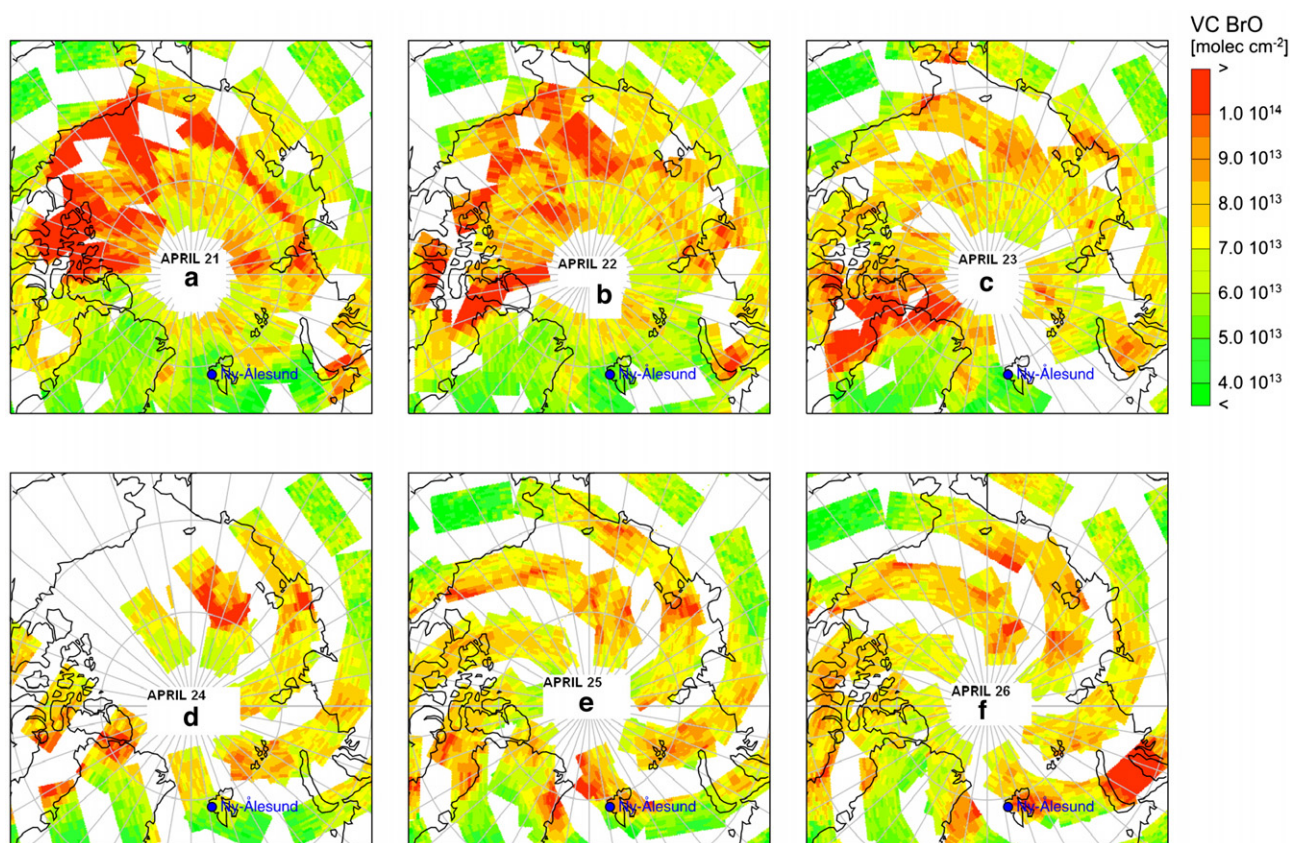


**Fig. 6** – Daily maps of the spatial distribution of BrO as derived from SCIAMACHY measurements for April 21 to 26, 2005. In places where several measurements were taken on the same day, the largest value is shown. The blue circle indicates the location of Ny-Ålesund. (For interpretation of the references to colour in this figure legend, the reader is referred to the web version of this article.)

#### 4.1.3. AMDE end period

During April 27 at night, GEM and O<sub>3</sub> concentrations began to increase again. Air masses associated with the end of the AMDE originated from the North Pole (see Fig. 5).

#### 4.1.4. Chemical mechanisms involved in the AMDE

The AMDE observed in this study was probably the result of already depleted air masses. According to Rankin et al. (2002) and Kaleschke et al. (2004), it is well known that frost flowers are a source of Br<sup>-</sup> anions and play a key role in bromine radical formation via Br<sub>2</sub> formation and its subsequent photolysis. These active bromine radicals contribute to ozone and mercury depletions. Thus BrO could be formed in areas covered by frost flowers (notably by the reaction between Br radical and O<sub>3</sub>). When comparing the BrO maps in Fig. 6 to the Potential Frost Flower (PFF) formation maps (Fig. 7), the fact that air masses recorded at Ny-Ålesund during the AMDE have high BrO concentrations because they flew over zones covered by frost flowers (Fig. 3) becomes evident. However the frost flowers were probably not the only bromine source for the AMDE. Two snowfall events were also observed during the AMDE (April 24 in the morning and from April 25 in the evening to April 26 at mid-day). As previously postulated by Ariya et al. (2004), Gauchard et al. (2005) and Glasow and Crutzen (oral communication), ice clouds at the origin of the snow fall could be involved in active

bromine production. Ice crystals, especially dendrites, formed in these clouds are good surfaces for heterogeneous reactions that allow sea salt aerosols containing Br<sup>-</sup> ions to produce active bromine species. It is therefore likely that frost flowers and ice clouds were the sources of BrO and active radical formation that led to both ozone and GEM depletion.

RGM and PM concentrations remained relatively low throughout the period of study (maximum values were ~50 pg/m<sup>3</sup> for PM and ~33 pg/m<sup>3</sup> for RGM). Higher levels were reported for this site in 2003 (~200 pg/m<sup>3</sup> for RGM and PM; Aspmo et al., 2005; Gauchard et al., 2005), but our 2005 Hg measurements are in good agreement with the values recorded by Berg et al. (2003) at Zeppelin (maximum concentrations were ~47 pg/m<sup>3</sup> for PM and ~12 pg/m<sup>3</sup> for RGM). These low concentrations suggest that deposition of RGM and PM occurred during air mass travel, thus supporting the hypothesis that the air mass was already depleted when it arrived at Ny-Ålesund.

#### 4.2. Snow to air interactions for Hg: what more have we learned?

##### 4.2.1. Diurnal cycle of Hg production and oxidized species deposition

Surface snow Hg concentrations measured during this field campaign showed very original results. Hg<sub>r</sub> concentrations in



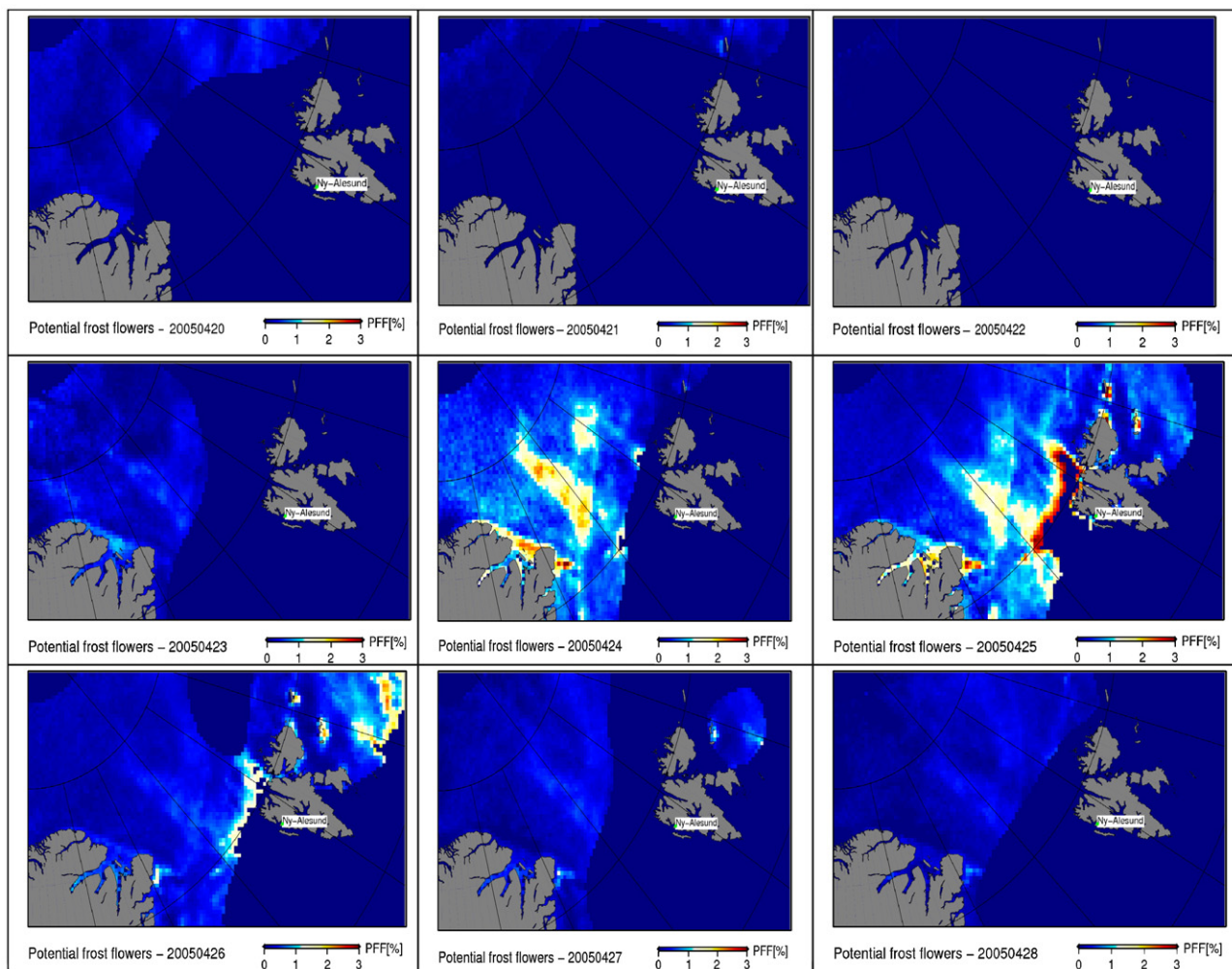


**Fig. 7 – Daily maps of Potential Frost Flowers (PFF) presented in chronological order from April 20 to April 28. Frost Flowers are located in the red zones while blue zones represent areas not covered by Frost Flowers. (For interpretation of the references to colour in this figure legend, the reader is referred to the web version of this article.)**

surface snow samples were systematically higher in the evening than in the morning (see Table 1). The average  $Hg_T$  concentration for mornings was  $\sim 23.5$  ng/L ( $\sigma = 12.8$  ng/L;  $n = 6$ ) and  $\sim 45.4$  ng/L ( $\sigma = 13.6$  ng/L;  $n = 6$ ) for evenings. Steffen et al. (2005) and Lahoutifard et al. (2005) reported diurnal variations in GEM concentrations above the snow pack that were correlated to snow to air fluxes of Hg and solar irradiation. This GEM diurnal cycle, with a maximum concentration at mid-day and a minimum at night, has also been observed in the present study. This GEM cycle could be attributed to the direct photoreduction of mercury complexes found in the surface snow (Lalonde et al., 2002; Dommergue et al., 2003). Sommar et al. (2004) have shown that in the atmosphere of Ny-Ålesund in the spring, BrO concentrations had the same pattern as GEM concentrations during the day with a maximum at mid-day. Furthermore, the same RGM diurnal pattern was observed in Barrow by Brooks et al. (2006), with a maximum at mid-day in the air at the snow surface. GEM maximum at mid-day is linked to re-emission from the snow while RGM production seems to be linked with GEM oxidation by Br/BrO radicals. So why do we observe a decrease in Hg

concentrations in the surface snow during the night? Two concurrent processes occurred in the first centimeters above the snow: GEM oxidation and RGM deposition. GEM was oxidized by bromine radicals (Br and BrO) and the oxidation maximum occurred at mid-day when bromine radical concentrations were at a maximum, which led to peak RGM levels. This RGM, formed in the first centimeters above the snow, was immediately deposited onto the snow surface where it could then be re-emitted back to the atmosphere via reduction processes. During the day, the chemical reaction that formed RGM and redeposited it onto the snow was probably faster than re-emission, leading to a net increase in Hg concentrations in the surface snow. Once irradiation decreased during the afternoon, production of active bromine radicals decreased, which led to a decrease in RGM formation and thus a reduction in RGM deposition onto the snow. Even if the re-emission flux was higher during the day (see Fig. 2d) with a maximum at mid-day, the surface snow still accumulated Hg as observed in Table 1. During the night, re-emission decreased to lower fluxes of about  $\sim 0.5$ – $1.0$  ng/m<sup>2</sup>/h. The GEM flux from the snow to the atmosphere contributed to reducing



Hg concentrations in the surface snow at night. This reduction is enhanced since RGM production and deposition are strongly reduced during the night. During the day, the “chemical engine” is shifted towards the formation of oxidized species of Hg and their deposition, thus increasing Hg concentrations in the surface snow.

#### 4.2.2. Hg deposition onto snow

Before the depletion, Average  $Hg_T$  concentration in the snow was about  $\sim 25.3$  ng/L ( $\sigma = 13.1$  ng/L;  $n = 7$ ) with a maximum of  $\sim 40$  ng/L (see Fig. 4). During the depletion, average  $Hg_T$  concentration reached  $\sim 44.1$  ng/L ( $\sigma = 19.0$  ng/L;  $n = 6$ ) and reached levels of up to  $\sim 90$  ng/L. After the depletion, the average concentration for  $Hg_T$  was 28.4 ng/L ( $\sigma = 18.5$  ng/L;  $n = 15$ ). It seems that the AMDE led to enhanced deposition of Hg onto snow surfaces. A 1.7 fold increase was recorded, which is low in comparison to what has previously been observed at other Arctic sites (Lu et al., 2001; Lindberg et al., 2002). In Ny-Ålesund, recent studies have shown lower Hg deposition increases during AMDEs (Berg et al., 2003; Ferrari et al., 2005) with the exception of a study by Sommar et al. (2004) who recorded concentrations of up to  $\sim 90$  ng/L. A similar level of  $Hg_T$  in the snow was recorded during the depletion event in this study, but just after a snow fall during the night of April 25 and the morning of April 26. It is possible that the oxidized mercury species formed in the atmosphere were trapped by the snow flakes and were deposited on the snow surface. The flakes formed in the clouds before the precipitation could also have been enriched in Hg since the air masses at the origin of the precipitation crossed through depleted air masses enriched in oxidized Hg species (Figs. 5–7). In our case, the increase in Hg in snow surface samples was the result of a strongly Hg enriched snow fall but not the result of dry RGM and PM deposition (Lindberg and Stratton, 1998).

#### 4.2.3. Fate of deposited Hg

What is the fate of Hg once deposited onto the snow pack? According to the results from our study, we observe four different periods for snow to air Hg fluxes. From April 14, 2005 to April 25, 2005, the emission flux stayed below  $4$  ng/m<sup>2</sup>/h and

the flux profile was correlated to solar irradiation with maximum flux at mid-day. From April 26, 2005 to April 29, 2005, GEM flux increased to reach maximum numbers close to  $10$  ng/m<sup>2</sup>/h. From April 29 to May 1, 2005, the fluxes peaked to  $\sim 35$  ng/m<sup>2</sup>/h. After May 2, 2005, GEM fluxes stayed below  $4$  ng/m<sup>2</sup>/h. The higher flux periods (e.g. from April 26, 2005 to May 1, 2005) corresponded to the AMDE in addition to the period following the event, when wind speed was low. We also observed two patterns for RGM and PM throughout the period of April 26 to April 30. PM peaked to  $\sim 50$  pg/m<sup>3</sup> on April 26 while RGM peaked to  $\sim 30$  pg/m<sup>3</sup> on April 28. It is likely that the nature of the Hg deposited during the AMDE had an effect on the PM and RGM deposition profiles. The three day maximum flux of  $\sim 10$  ng/m<sup>2</sup>/h corresponded to the period where RGM and PM concentrations were maximum. It seems that the deposition of RGM and PM from the atmosphere led to an increase in GEM flux from the snow to the atmosphere as a result of direct or photoinitiated reduction (Dommergue et al., 2003; Ferrari et al., 2005; Aspino et al., 2006; Kirk et al., 2006). But the two day high fluxes (up to  $35$  ng/m<sup>2</sup>/h) corresponded to low PM and RGM concentration periods. This period was characterized by an increase in snow temperature (see Fig. 8a). Dommergue et al. (2003) showed that the snow pack, when it is close to melting, emits more GEM than when temperatures are lower. The higher emission fluxes recorded in the present study could therefore be the result of this increase in snow temperature, which leads to a metamorphism of snow and an increase in the water layer around snow grains, consequently augmenting GEM production in the snow (Ferrari et al., 2005). The decrease in wind speed contributed to increasing the recorded flux. Finally we can estimate that 80% of the deposited Hg during the depletion was reemitted back to the atmosphere in the days following the event.

#### 4.2.4. Evolution of Hg content in surface snow

Both  $Hg_T$  and  $Hg_R$  concentrations were measured in the snow. We consider the concentration of stable Hg as the difference between  $Hg_T$  and  $Hg_R$  concentrations. Fig. 8 shows the ratio between the stable concentration vs.  $Hg_T$  concentration as a function of snow temperature. The ratio stayed low when the

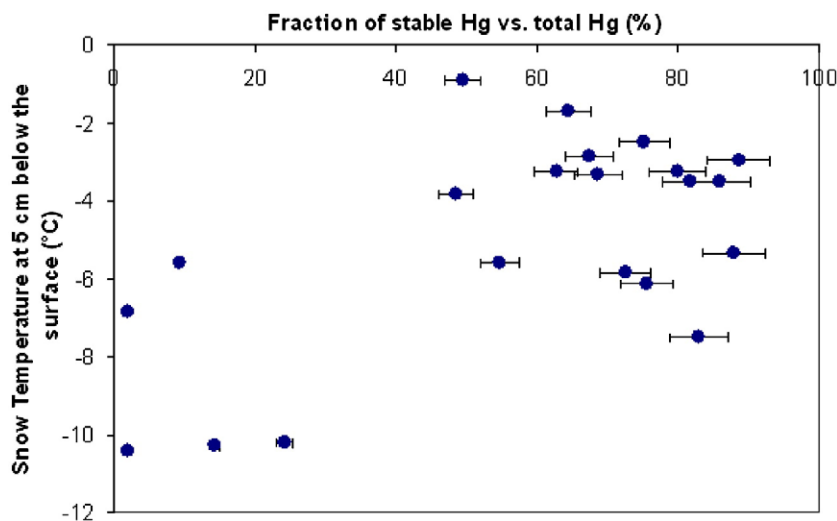


Fig. 8 – Fraction of stable Hg vs.  $Hg_T$  as a function of snow temperature (°C).

snow temperature was low, but increased with snow temperature, especially when the snow was close to melting. Two hypotheses can be given to explain such profile. First, the reactive Hg complexes can be sorbed onto particles or aerosols when the snow morphology changes as the temperature increases. In the liquid layers around crystal grains, mercury can bind strongly to particle surfaces (Landis et al., 2002) leading to stabilized mercury complexes which are not measured as Hg<sub>R</sub> with our technique. The second explanation could be linked to microbial activity in the liquid layer around snow grains when the temperature increases. Polar bacteria, and especially those from the Ny-Ålesund snow pack (see Amato et al., 2006 for details), were shown to interact strongly with mercury at concentrations close to those measured during this campaign (Hennebelle et al., 2006). Finally, as snow temperature increases, bacteria can grow and divide rapidly. This growth period could also be a period where strains (e.g. bacteria, fungi, yeast) generate exopolysaccharides (EPS) (Krembs, 2006) that are known to interact with heavy metals to form compounds (Loaëc et al., 1998), which cannot be measured as Hg<sub>R</sub> with our technique.

## 5. Summary and conclusion

A field campaign was held in Ny-Ålesund, Svalbard (Norway) in order gain insights on Atmospheric Mercury Depletion Events (AMDE) in the Arctic. An AMDE, which lasted over 3 days and led to a net increase (2 fold) in Hg deposition onto snow surfaces, was observed. The origin of this AMDE seems to be linked to the transport of already depleted air masses as shown by both SCIAMACHY BrO data and Potential Frost Flowers (P.F.F.) maps. The increase in Hg deposition appears to be linked directly to a snow fall event, which leads us to the hypothesis that in-cloud atmospheric oxidation of GEM is an important deposition process for oxidized mercury. In this study, we also demonstrated that both oxidation and reduction processes occurred at the snow surface interface, leading to mercury deposition and GEM emission. This has been demonstrated by the diurnal cycle in Hg concentrations in the surface snow samples. The fraction of Hg<sub>R</sub> mercury in snow seems to decrease strongly as spring progresses. This may possibly be related to changes in snow characteristics, especially as the snow becomes more and more wet. In the liquid space around snow grains, Hg<sub>R</sub> can interact with organic matter, thus generating a more stable mercury form which is not analyzed as Hg<sub>R</sub>. If this process, which requires more investigation, is verified, it could have an important environmental impact. Since the stabilized mercury form may have a longer lifetime in snow and melted water, then the likelihood of it being introduced into polar systems increases, thereby contributing to environmental mercury contamination.

## Acknowledgements

This research was funded by the French polar Institute I.P.E.V. [Institut Paul-Emile Victor, program CHIMERPOL 399], the A.D. E.M.E. (Agence de l'Environnement et de la Maîtrise de l'Energie, Programme 0162020), the French Ministry of Environ-

ment and Sustainable Development, the French ministry of research (ACI 3012) and the CNRS [Centre National de la Recherche Scientifique]. Claude Boutron and Christophe Ferrari thank the Institut Universitaire de France (I.U.F.) for its financial help for this research. We thank Franck Delbart, Martin Mellet and Nicolas Le Viavant from the I.P.E.V. for their constant help during the field experiments. We would like to express our thanks to the Alfred Wegener Institute (A.W.I) and especially the Koldewey station and its staff, the Norwegian Polar Institute and the Kings Bay for their help during our stay.

## REFERENCES

- Amato P, Hennebelle R, Magand O, Sancelme M, Delort A-M, Barbante C, et al. Bacterial characterization of the snow cover in Svalbard, Spitzberg. *FEMS microbiol Ecol* 2006;59:255–64.
- Ariya PA, Dastoor AP, Amyot M, Schroeder WH, Barrie L, Anlauf K, et al. The Arctic: a sink for mercury. *Tellus B* 2004;56:397–403.
- Aspmo K, Gauchard P-A, Steffen A, Temme C, Berg T, Bahlmann E, et al. Measurements of atmospheric mercury species during an international study of mercury depletion events at Ny-Alesund, Svalbard, spring 2003. How reproducible are our present methods? *Atmos Environ* 2005;39:7607–19.
- Aspmo K, Temme C, Berg T, Ferrari C, Gauchard P-A, Fain X, et al. Mercury in the atmosphere, snow and melt water ponds in the North Atlantic Ocean during Arctic summer. *Environ Sci Technol* 2006;40(13):4083–9.
- Berg T, Sekkeseter S, Steinnes E, Valdal A-K, Wibetoe G. Springtime depletion of mercury in the European Arctic as observed at Svalbard. *Sci Total Environ* 2003;304:43–51.
- Brooks SB, Saiz-Lopez A, Skov H, Lindberg SE, Plane JMC, Goodsite ME. The mass balance of mercury in the springtime arctic environment. *Geophys Res Lett* 2006;33:L13812. doi:10.1029/2005GL025525.
- Dommergue A, Ferrari CP, Gauchard P-A, Boutron CF, Poissant L, Pilote M, et al. The fate of mercury species in a sub-arctic snow-pack during snowmelt. *Geophys Res Lett* 2003;30:1621. doi:10.1029/2003GL017308.
- Ebinghaus R, Kock H, Temme C, Einax J, Löwe A, Richter A, et al. Antarctic springtime depletion of atmospheric mercury. *Environ Sci Technol* 2002;36:1238–44.
- Fain X, Ferrari CP, Gauchard P-A, Magand O, Boutron C. Fast depletion of elemental gaseous mercury in the Kongsvegen Glacier snowpack in Svalbard. *Geophys Res Lett* 2006;33:L06826. doi:10.1029/2005GL025223.
- Fain X, Grangeon S, Fritsche J, Bahlmann E, Obrist D, Ferrari C P. Diurnal production of gaseous mercury in the alpine snowpack before snowmelt. *J Geophys Res* 2007;112:D21311. doi:10.1029/2007JD008520.
- Ferrari CP, Gauchard PA, Aspmo K, Dommergue A, Magand O, Bahlman E, et al. Snow-to-air exchanges of mercury in an Arctic seasonal snow pack in Ny-Ålesund, Svalbard. *Atmos Environ* 2005;39:7633–45.
- Gauchard PA, Aspmo K, Temme C, Steffen A, Ferrari CP, Berg T, et al. Study of the origin of atmospheric mercury depletion events recorded in Ny-Ålesund, Svalbard, spring 2003. *Atmos Environ* 2005;39:7620–32.
- Kaleschke L, Richter A, Burrows J, Afe O, Heygster G, Notholt J, et al. Frost flowers on sea ice as a source of sea salt and their influence on tropospheric halogen chemistry. *Geophys Res Lett* 2004;31:L16114.
- Kirk JL, St. Louis VL, Sharp MJ. Rapid reduction and reemission of mercury deposited into snowpacks during atmospheric mercury depletion events at Churchill, Manitoba, Canada. *Environ Sci Technol* 2006;40(24):7590–6.

- Krembs C. Seasonal evolution of exopolymeric substances and their significance for the annual sea-ice productivity. International conference on alpine and polar microbiology, Innsbruck, Austria; 2006. 27–31th March.
- Lalonde JD, Poulain AJ, Amyot M. The role of mercury redox reactions in snow on snow-to-air mercury transfer. *Environ Sci Technol* 2002;36(2):174–8.
- Lahoutifard N, Sparling M, Lean D. Total and methyl mercury patterns in Arctic snow during springtime at Resolute, Nunavut, Canada. *Atmos Environ* 2005;39:7597–606.
- Landis MS, Stevens R, Schaedlich F, Prestbo E. Development and characterization of an annular denuder methodology for the measurement of divalent inorganic reactive gaseous mercury in ambient air. *Environ Sci Technol* 2002;36:3000–9.
- Lindberg SE, Stratton WJ. Atmospheric mercury speciation: concentrations and behaviour of reactive gaseous mercury in ambient air. *Environ Sci Technol* 1998;32:49–57.
- Lindberg SE, Brooks S, Lin C-J, Scott KJ, Landis MS, Stevens RK, et al. Dynamic oxidation of gaseous mercury in the arctic troposphere at polar sunrise. *Environ Sci Technol* 2002;36:1245–56.
- Lindqvist O, Rhode H. Atmospheric mercury—a review. *Tellus* 1985;37B:136–159.
- Loaëc M, Olier R, Guezennec J. Chelating properties of bacterial exopolysaccharides from deep sea hydrothermal vents. *Carbohydr Polym* 1998;35:65–70.
- Lu JY, Schroeder WH, Barrie LA, Steffen A, Welch HE, Martin K, et al. Magnification of atmospheric mercury deposition to polar regions in springtime: the link to tropospheric ozone depletion chemistry. *Geophys Res Lett* 2001;28:3219–22.
- Munthe J, Kindbom K, Kruger O, Petersen G, Pacyna J, Iverfeldt A. Examining source-receptor relationships for mercury in Scandinavia. Modelled and empirical evidence. *Water Air Soil Pollut., Focus* 2001;1(3–4):299–310.
- Planchon F, Gabrielli P, Gauchard PA, Dommergue A, Barbante C, Cairns WRL, et al. Direct determination of mercury at the sub-picogram per gram level in polar snow and ice by ICP-SFMS. *J Anal At Spectrom* 2004;19:823–30.
- Poissant L, Pilote M. Atmospheric mercury and ozone depletion events observed at low latitude along the Hudson Bay in northern Quebec (Kuujuaarapik: 55°N). Presented at the 6th International Conference on Mercury as a Global Pollutant, Minamata, Japan; 2001.
- Rankin AM, Wolff EW, Martin S. Frost flowers: implications for tropospheric chemistry and ice core interpretation. *J Geophys Res* 2002;107:4683–97.
- Richter A, Wittrock F, Eisinger M, Burrows JP. GOME observations of tropospheric BrO in Northern Hemispheric spring and summer 1997. *Geophys Res Lett* 1998;25:683–2686.
- Skov H, Christensen J, Goodsite M, Heidam NZ, Jensen B, Wählin P, et al. Fate of elemental mercury in the Arctic during atmospheric mercury depletion episodes and the load of atmospheric mercury to the Arctic. *Environ Sci Technol* 2004;38:2373–82. doi:10.1021/es030080h.
- Slemr F, Schuster G, Seiler W. Distribution, speciation, and budget of atmospheric mercury. *J Atmos Chem* 1985;3:407–34.
- Slemr F, Brunke EG, Ebinghaus R, Temme C, Munthe J, Wängberg I, et al. Worldwide trend of atmospheric mercury since 1977. *Geophys Res Lett* 2003;30 Art No 1516.
- Sommar J, Wängberg I, Berg T, Gardfeldt K, Munthe J, Richter A, et al. Circumpolar transport and air-surface exchange of atmospheric mercury at Ny-Alesund (79° N), Svalbard, spring 2002. *Atmos Chem Phys Discuss* 2004;4:1727–71.
- Steffen A, Schroeder WH, Bottenheim J, Narayana J, Fuentes JD. Atmospheric mercury concentrations: measurements and profiles near snow and ice surfaces in the Canadian Arctic during Alert 2000. *Atmos Environ* 2002;36:2653–61.
- Steffen A, Schroeder W, Macdonald RW, Konoplev A. On-going atmospheric mercury measurements in the high Arctic in Canada and Russia. *Mater Geo-environ* 2004;51:1786–90.
- Steffen A, Schroeder WH, Macdonald R, Poissant L, Konoplev A. Mercury in the arctic atmosphere: an analysis of eight years of measurements of GEM at Alert (Canada) and a comparison with observations at Amderma (Russia) and Kuujuaarapik (Canada). *Sci Total environ* 2005;342:185–98.
- Temme C, Einax J, Ebinghaus R, Schroeder W. Measurements of atmospheric mercury species at a coastal site in the Antarctic and over the South Atlantic Ocean during polar summer. *Environ Sci Technol* 2003;37:22–31.
- Tuckermann M, Ackermann R, Götz C, Lorenzen-Schmidt H, Senne T, Stutz J, et al. DOAS-observation of halogen radical-catalysed arctic boundary layer ozone destruction during the ARCTOC-campaigns 1995 and 1996 in Ny-Alesund, Spitsbergen. *Tellus* 1997;49B:533–55.
- Wittrock F. The retrieval of oxygenated volatile organic compounds by remote sensing techniques. Bremen: University of Bremen; 2006. 192 pp., <http://nbn-resolving.de/urn:nbn:de:gbv:46-diss000104818>.
- Wittrock F, Oetjen H, Richter A, Fietkau S, Medeke T, Rozanov A, et al. MAX-DOAS measurements of atmospheric trace gases in Ny-Alesund — radiative transfer studies and their application. *Atmos Chem Phys* 2004;4:955–66.